



This is a repository copy of *Prediction of the impact of thermal cycling on machine lifetime based on accelerated life testing and finite element analysis*.

White Rose Research Online URL for this paper:

<https://eprints.whiterose.ac.uk/201860/>

Version: Accepted Version

---

**Proceedings Paper:**

Hewitt, D. [orcid.org/0000-0002-4585-2915](https://orcid.org/0000-0002-4585-2915) and Wang, J. [orcid.org/0000-0003-4870-3744](https://orcid.org/0000-0003-4870-3744) (2021) Prediction of the impact of thermal cycling on machine lifetime based on accelerated life testing and finite element analysis. In: IECON 2021 – 47th Annual Conference of the IEEE Industrial Electronics Society. IECON 2021 - 47th Annual Conference of the IEEE Industrial Electronics Society, 13-16 Oct 2021, Toronto, ON, Canada. IEEE , pp. 1-6. ISBN 9781665435543

<https://doi.org/10.1109/iecon48115.2021.9589387>

---

© 2021 IEEE. Personal use of this material is permitted. Permission from IEEE must be obtained for all other users, including reprinting/ republishing this material for advertising or promotional purposes, creating new collective works for resale or redistribution to servers or lists, or reuse of any copyrighted components of this work in other works. Reproduced in accordance with the publisher's self-archiving policy.

**Reuse**

Items deposited in White Rose Research Online are protected by copyright, with all rights reserved unless indicated otherwise. They may be downloaded and/or printed for private study, or other acts as permitted by national copyright laws. The publisher or other rights holders may allow further reproduction and re-use of the full text version. This is indicated by the licence information on the White Rose Research Online record for the item.

**Takedown**

If you consider content in White Rose Research Online to be in breach of UK law, please notify us by emailing [eprints@whiterose.ac.uk](mailto:eprints@whiterose.ac.uk) including the URL of the record and the reason for the withdrawal request.



[eprints@whiterose.ac.uk](mailto:eprints@whiterose.ac.uk)  
<https://eprints.whiterose.ac.uk/>

# Prediction of the Impact of Thermal Cycling on Machine Lifetime Based on Accelerated Life Testing and Finite Element Analysis

David Hewitt

Department of Electronic and Electrical Engineering,  
University of Sheffield,  
Sheffield  
David.Hewitt@Sheffield.ac.uk

Jiabin Wang

Department of Electronic and Electrical Engineering,  
University of Sheffield,  
Sheffield  
j.b.wang@sheffield.ac.uk

*Electric machines are constructed from a variety of different materials which exhibit different mechanical and thermal expansion properties. Losses within the machine cause an increase in temperature, resulting in thermally induced internal stresses in insulation materials. Changes to the operating condition will result in different levels of loss being produced, and give rise to a thermal cycling profile to the machine and cyclic stress in the insulation. This paper studies the impact of these thermal cycles and resultant cyclic stress in the insulation on the lifetime of machines. Through the use of finite element analysis the internal stress levels, and corresponding stress cycle profiles are determined within the machine insulation layer, this data is then combined with experimental data, allowing stress-life (number of cycles) (SN)-curves to be generated for the machine type under test. The correlation between predicted insulation fatigue life with the measurements provides a physical insight of lifetime reduction due to thermal cycling.*

**Keywords**—*Electric Machines, Lifetime Estimation, Accelerated Aging, Finite Element Analysis*

## I. INTRODUCTION

Electric machines are constructed from a combination of different materials which exhibit different mechanical and thermal expansion properties. Due to losses within the machine (copper loss, iron loss and mechanical loss, etc.) the temperature of the machine will change during operation. Mismatches between materials mechanical properties, particularly the thermal expansion coefficient, will result in thermally induced internal stresses occurring within the components, and at the interfaces between these components. The induced mechanical stress within insulation coatings of magnet wire conductors is of particular concern.

In a variety of emerging applications, such as electrical drives in electrified transport, it is likely that the machine will not be operated at a constant loading. Hence variations in loading will result in corresponding variations in machine losses and consequently variations in temperatures, causing the mechanical stress to vary with respect to the machine loading levels. This causes cyclic stresses within the insulation coatings.

In [1] and [2] finite elements simulations are utilised to predict the levels of stress which occur in windings due to thermal mismatch within single conductors and bundle analogues. This work demonstrates that the level of thermal stress which occurs within encapsulated windings is significant. In this work, lifetime predictions are made based

on the manufacturer's material data, which is generated using mechanically applied stresses, rather than thermal mismatch. In [3] and [4] the authors consider the impact of mechanical stress cycling on material samples, with a view to demonstrating the detrimental impacts of cycling on lifetime. Of particular interest in both of these papers is the demonstration that failure can occur within components at stress levels which do not exceed the yield/ultimate tensile strength of the material.

Experimental work has previously been carried out to determine the impact of thermal cycling on electric machines [5]. In this work, sample machine stators were operated in elevated temperature environments under a range of cyclic loadings, so as to induce thermal cycling in the machines. The lifetime of these samples was then compared to samples which had not undergone cycling, allowing the effects of thermal cycling to be isolated and studied. The objective of this work is to use this experimental data, combined with finite element analysis (FEA) to generate data suitable for use in lifetime estimation for the tested machine. This differs from previous work presented in literature in that the life predications are based on experimental data for the material within a practical configuration (within a machine winding), consequently the experimental data will reflect the effects of this configuration on the lifetime, and is therefore likely to be more representative than data obtained under very different testing conditions.

This data may also be used for the basis of life estimation for machines of similar construction/material makeup. The correlation between predicted insulation fatigue life with the measurements provides a physical insight of lifetime reduction due to thermal cycling.

## II. EXPERIMENTAL METHODOLOGY

For reference, the process by which the experimental data was generated in [5] will be summarized here. In this work a total of eleven sample machine stators were tested. Of these samples four were operated at fixed temperatures of 205°C; 215°C; 230°C and 250°C; using this data, it is possible to determine the rate of thermal degradation of the machines under a constant temperature of operation. A further seven samples were tested under thermally cycling conditions, achieved by varying the magnitude of the stator current controlled by a 3-phase inverter. The inverter excitation is

maintained throughout the lifetime of a test sample. A summary of the cycling profiles are shown in TABLE I.

TABLE I THERMAL CYCLING PROFILES AND MEASURED CYCLE LIFETIMES

Sample	Peak Temp (°C)	Min Temp (°C)	$\Delta T$ (°C)	Cycles	% life due to thermal aging (%)	% life due to cycles (%)	Scaled Cycles
2	250	190	60	73	49	51	143
3	250	210	40	119	57	43	277
4	250	170	80	51	40	60	85
5	240	200	40	230	63	37	621
6	240	180	60	197	55	45	438
7	240	160	80	71	20	80	89

Over the course of testing, each sample was exposed to the cycling profile outlined in TABLE I, at a rate of one cycle every two hours. The minimum temperature of the machine was established by placing the sample inside a temperature controlled oven. Temperature cycling was then achieved by adjusting the magnitude of the current supplied to the machine windings, increasing and decreasing the machine temperature periodically.

Based on the temperature profile which the samples were exposed to it is possible to also calculate the percentage of life lost due to thermal aging over the course of the test; this is calculated with reference to the initial samples which were not exposed to cycling. Due to the conditions under which the tests were conducted, it is reasonable to assume that the remainder of the life lost by the machine was a product of the thermal cycling process. Using this assumption it is possible to scale the number of cycles to failure, to create a hypothetical scenario in which the machine is aged solely by the thermal cycling mechanism. While such a case can never physically exist, it is useful for comparison to FEA results, as the FEA simulation results will not account for the effects of chemically instigated thermal aging.

### III. FEA MODELLING

#### A. Design of FEA model

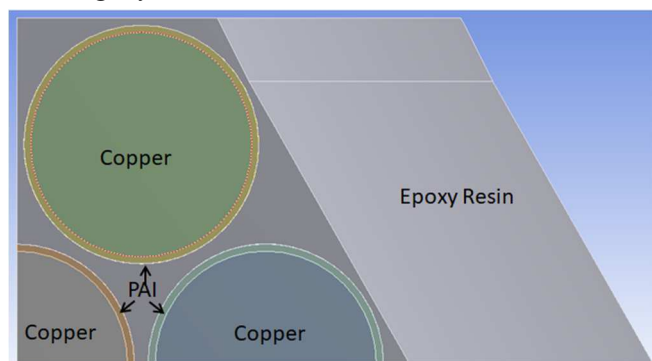


Fig. 1 Original hexagonal model used to simulate coating stress levels

In order to generate suitable stress-cycle (SN) curves it is necessary to quantify the level of stress which is present within the conductor coating layers of the machine windings at a given temperature. This can be calculated using FEA. To achieve this, a 3D finite element model was employed.

This model used 1/8<sup>th</sup> symmetry, and the hexagonal layout shown in Fig. 1. This model represents a typical conductor layout for conductors within a machine winding which have been encapsulated within epoxy resin. In this example, the conductors have a diameter of 0.8mm, and are coating in a layer of polyamide-imide (PAI) with a thickness of 0.025mm. Thermal excitation was applied to the model by setting the temperature of all volumes to the stated temperature. This model was simulated at a number of different temperatures, with a number of different conductor spacing values, representing a copper fill factor of 45% to 73%. The material data used in the assessment are listed in Table II.

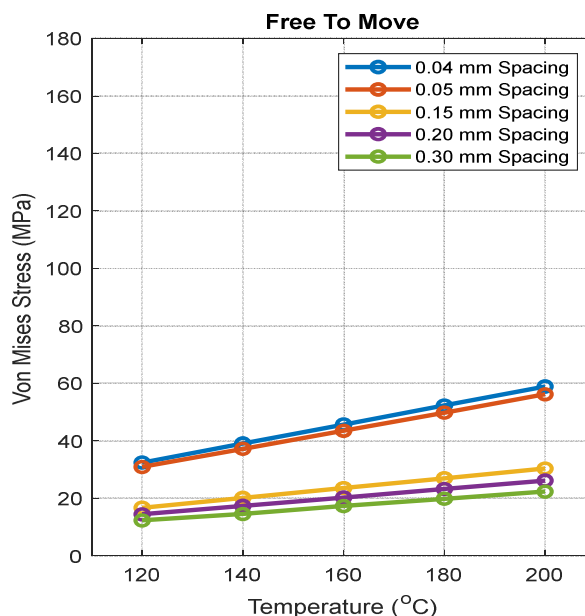


Fig. 2 Results of hexagonal model simulation with a free to move outer boundary

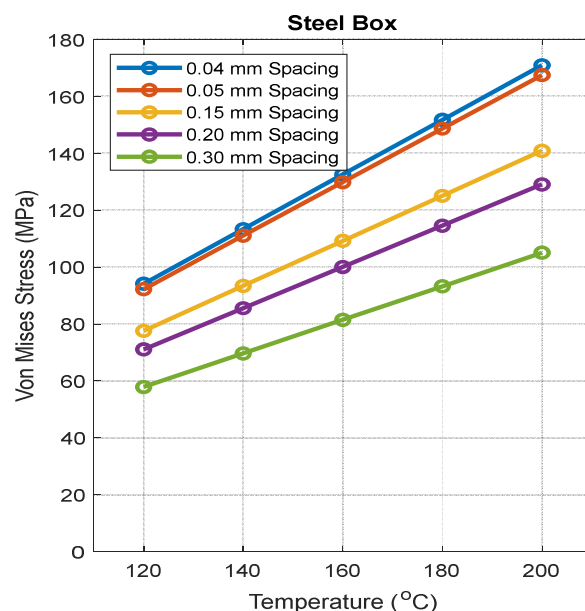


Fig. 3 Results of hexagonal model simulation with a steel layer constrained outer boundary

This model was also simulated with two different boundary conditions applied to the outer surfaces of the model. These

conditions were: free-to-move and constrained by a steel enclosure. It is expected that the practical case, of a bundle of conductors within a machine slot will fall somewhere between these two cases, the validity of this assumption is considered later in this paper. The results of these simulations can be observed in Fig. 2 and Fig. 3 respectively.

TABLE II MATERIAL PROPERTIES USED IN SIMULATION

	Young's Modulus (GPa)	Poisson's Ratio	Density (g/cm <sup>3</sup> )	CTE (μm/m.°C)	Thermal Cond (W/m.K)
4203L Coating	4.500	0.450	1.420	30.6	0.260
EIP 4260 Epoxy	3.500	0.440	1.730	70.0	0.600
Copper	110.0	0.340	8.300	18.0	401
Nomex 410	3.400	0.322	1.318	20.0	0.149
Polyester Resin	3.393	0.400	1.000	150	0.200

From these simulations it can be concluded that adding additional constriction to the conductors, by way of the external steel box, results in higher stresses within the conductor coatings. To determine which of these configurations is more representative it is desirable to produce a model which captures the topology of half a machine slot.

### B. Modelling a machine slot

A challenge which occurs when trying to produce a model of a whole machine slot is difference in scale between the slot geometry and the individual conductors, or more specifically, the insulation layer, on the surface of the conductors. Trying to produce a model which includes a large number of conductors, but which is also discretised with a sufficiently fine mesh to capture the behaviour of this coating is problematic. It is theorised that due to the small thickness of the coating layer relative to the overall model size, the impact of this layer on the simulation results will be quite small. However, as the coating layer is the area of specific interest in this work, the layer cannot be entirely eliminated from the model. As a compromise, it would be preferable to omit the coating layer for all conductors not being studied, while still including the layer on conductors which are being looked at.

To assess the viability of this approach the model shown in Fig. 4 is used. If this approach is to be used, it is necessary to determine if it is preferable to replace the coating layer with the surrounding epoxy material, or the copper of the conductor. The model was evaluated for both cases, with the results being compared with the normal model, in which the coating layer is represented by the coating material. For all three simulation cases, the Von-Mises stress within the coating of the conductor of interest (bottom left corner) is extracted from the middle of the coating layer, along a path which starts at the bottom edge of the model and ends at the left. The results of this are presented in Fig. 5. It can be observed from this figure, that replacing the coating material with the surrounding epoxy material, for the conductors not directly under study, has little impact on the stresses in the studied conductor coating. This shows that if this layer is to

be omitted, it is preferable to replace it with the epoxy material, rather than copper, as this minimises the impact on the conductor of interest.

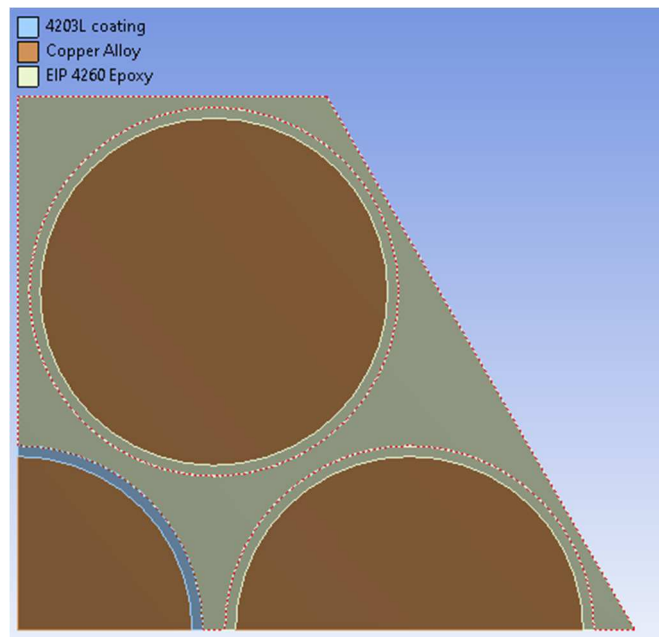


Fig. 4 Reduced coating model geometry

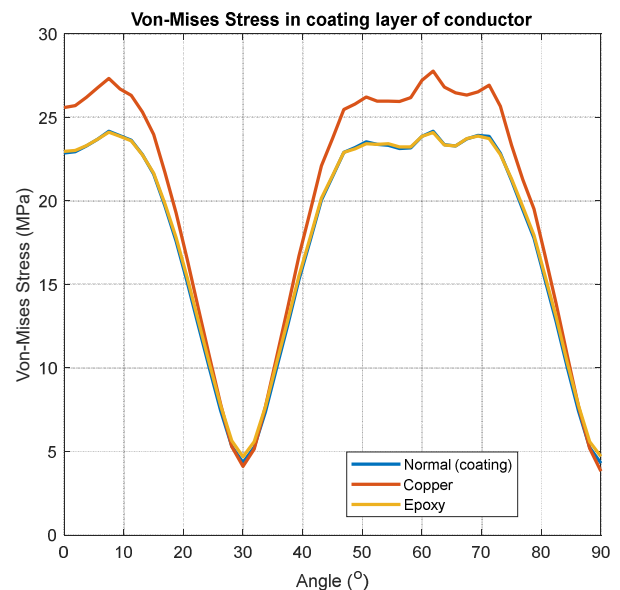


Fig. 5 Coating layer stress in conductor of interest with different materials applied to other conductors

### C. Hot-spot location

It has been shown in literature [6] that the peak coating layer stress occurs on the conductor which is located within the hot-spot of the slot. To identify this position of the hottest conductor the model shown in Fig. 6 is used. This model is produced using the same conductor geometry as the previously discussed hexagonal model. Due to the fact that the epoxy and coating material have similar thermal properties, the coating layers are omitted for all conductors during this analysis. To find the hotspot location, a current density of 9.95 A/mm<sup>2</sup> is applied to all of the conductors. To simulate the machine being cooled through the machine casing, the outer face of the machine is constrained to

150°C. The results of this simulation can be observed in Fig. 7. From this it can be seen that the peak temperature is 161.38°C in the position identified by the 'max' label.

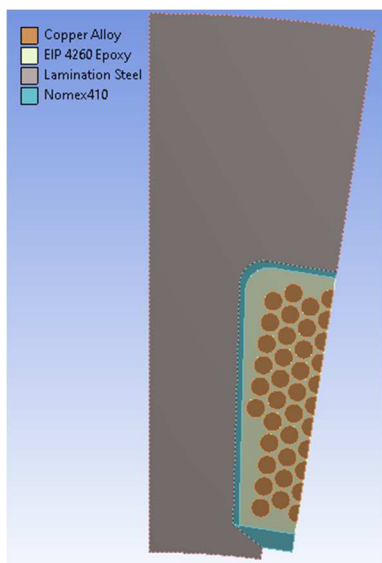


Fig. 6 – Half slot thermal model

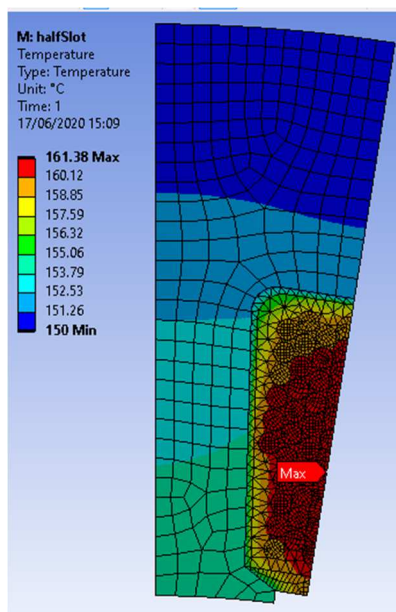


Fig. 7 Thermal profile of half slot model

Based on this result the model was modified to include a coating layer on this conductor. This model was then solved for a range of different temperatures, with the peak coating stress value being extracted for each case. In these simulations, the thermal excitation was supplied to the model by setting the temperature of the whole model to the specified temperature. This was done to allow the results from this model to be directly compared with the previously discussed results from the hexagonal models.

Fig. 8 shows the stress distribution within the coating of the conductor identified as the hot-spot conductor in the previous analysis. The distribution of this stress is comparable to the stress distribution observed in the hexagonal models, whereby the peak stress occurs in line with the adjacent conductors within the slot.

In Fig. 9 the peak coating stress values from the half slot model are compared to the values obtained from the hexagonal models, with both types of boundaries. It can be observed that the free-to-move and half slot models show only a ~15% deviation. It can be seen from the figure that this case is much more representative of the half slot data than the alternative, steel surrounded case. Suggesting that the steel constrained boundary imparts considerably more stress to the conductors under study than can be expected to be the typical case in a machine slot.

Based on these results, the free-to-move case is more representative than the constrained case. For this reason the free-to-move case will be used throughout the remainder of this study.



Fig. 8 Stress distribution within conductor coating (Temperature = 200°C) (Units = Pa)

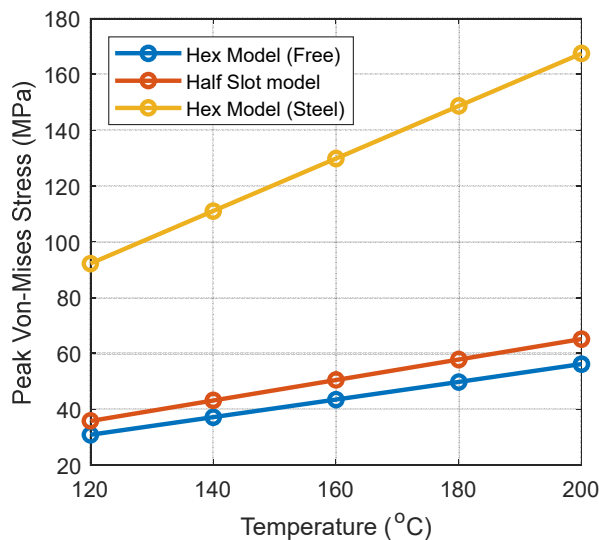


Fig. 9 Comparison between different boundary conditions and half slot model

#### D. Topology in test machine

To generate data suitable for use with the published experimental data it is necessary to re-work the hexagonal model to ensure that the conductor geometry used matches that of the machine under study. To this end the model shown in Fig. 10 was created. This model is produced in the same way as the previously discussed hexagonal models, using the conductor size, coating thickness and potting

material values which match those of the test samples. The peak coating stress values, at a range of temperatures, for a range of conductor spacing values are shown in Fig. 11. These stress values can be combined with the scaled experimental data to produce an SN-curve suitable for machine life prediction under cycling conditions.

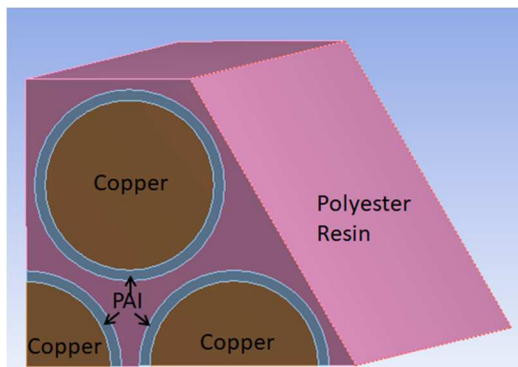


Fig. 10 Hexagonal model of machine under test in experimental work

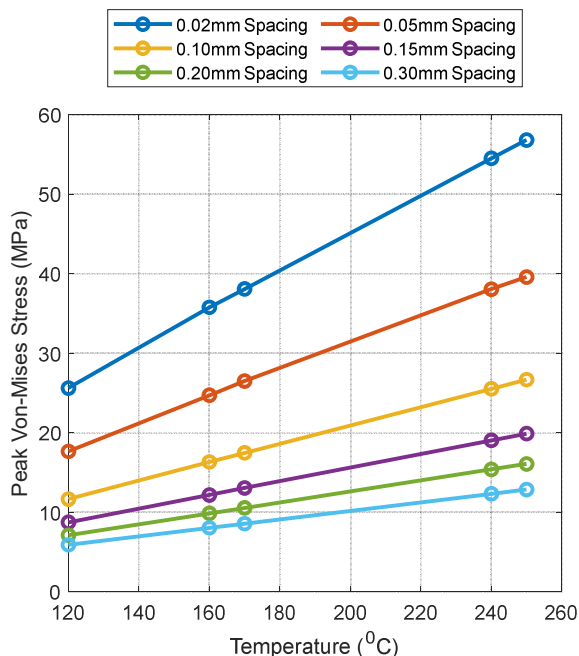


Fig. 11 Peak coating stress values for simulated test machine, for a range of wire spacing values and temperatures

#### IV. LIFE PREDICTION

When lifetime data is provided by material manufacturers it is relatively common that the data which is supplied relates to testing under fully reversed stress conditions. For this to be the case, the stress values which are applied to the sample will vary between the values of +/-Peak Stress. Using the FEA model of the windings it is possible to determine the minimum and maximum coating stress values for each sample. These values can be processed using mean stress correction theory to calculate the equivalent fully reversed stress values for each experimental sample. In the case of this work the Goodman method is employed, using an ultimate tensile strength (UTS) value of 66.44MPa (Obtained by extrapolating the values from the material datasheet to obtain the value at 250°C) for the coating material. By plotting the calculated stress values against the experimentally scaled cycle values, it is possible to generate

an SN-curve for the machines under test. The result of this, considering a range of different conductor spacing values, can be observed in Fig. 12. When presented on a log-log scale, it is expected that the data should appear as a straight line. In Fig. 12 the fitted curves are generated using equation (1), where  $S$  is the Stress value;  $cycles$  is the number of cycles; and  $a$  and  $b$  are empirical constants.

$$S = a \text{ cycles}^b \quad (1)$$

Of particular interest in this dataset are the values obtained for spacing values of 0.02mm and 0.05mm. If a stress greater than or equal to the ultimate tensile strength is applied to a material, it is expected that the material will fail without the effects of cycling (or put another way, failure occurs at one cycle). To this end, it is expected that the fitted curve should have a value close to the UTS value at 1 cycle. Particularly in the 0.02mm case this is true; with the fitted curve actually intersecting the UTS value at ~4 cycles. Furthermore, in this case, the experimental data exhibits good clustering around the fitted curve.

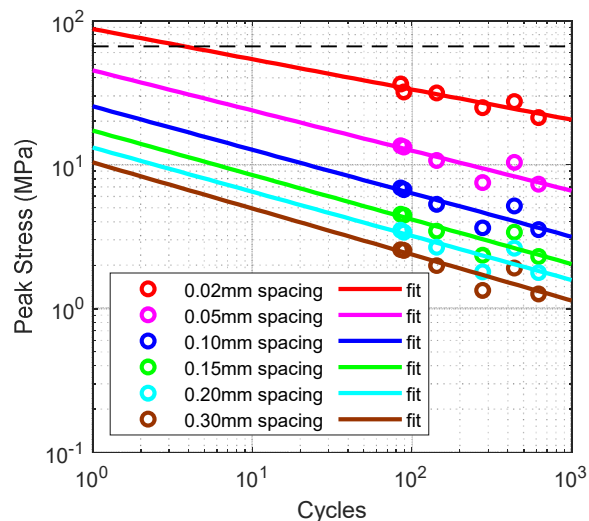


Fig. 12 Goodman Mean stress corrected values for experimental samples (UTS = 66.44MPa)

To evaluate the validity of the SN-curve generated using FEA/experimental data it is useful to compare it to the material data for polyamide-imide (PAI) provided by a material manufacturer (Torlon 4203L) [7]. While the exact variant of insulation material is not known for the machine samples, this data should give a good indication for the material. The comparison between the manufacturers data and the 0.02mm spacing data can be observed in Fig. 13. When considering this data there are a few points which are worth noting, which potentially explain discrepancies between the datasets.

Firstly, by observing the trends in the manufactures data it can be seen that the cycle endurance of the material decreases as temperature increases. As the generated cycling data was obtained at peak temperatures of 240/250°C, it is reasonable to expect that this data would show much lower cyclic endurance for a given stress level. A further point to note is the difference between the methods used to generate the data sets. In the case of the manufacturer supplied

information, the data is generated using a solid piece of material, which is exposed to mechanical stress at a given temperature. This differs from the experimental data generated in this work, whereby the stress is applied to the sample through thermal expansion using temperature variation and the samples are thin films applied to copper conductors within a machine winding.

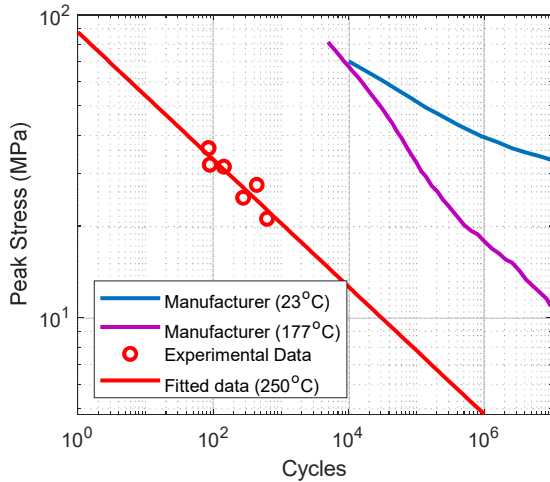


Fig. 13 Comparison of generated SN-curve and manufacturers data

#### V. APPLICATION TO LOWER TEMPERATURE OPERATION

Using the previously discussed FEA model it is possible to simulate the stress within the coating layer for any peak temperature/temperature cycle. Using the results of this simulation it is possible to predict the lifetime of the machine using the generated SN curve.

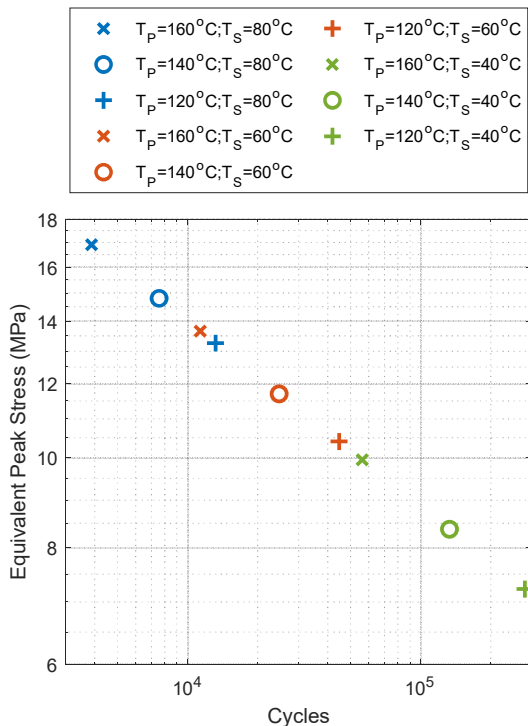


Fig. 14 Predicted lifetime for machines with lower temperature values (Where  $T_p$  is the Peak temperature and  $T_s$  is the temperature swing)

To explore this, three different peak temperatures – 120; 140 and 160°C were considered. For each of these temperature values, temperature swings of 40; 60 and 80°C were evaluated. For each case the equivalent stress was calculated, this value was then applied to the SN curve

generated using 0.02mm spacing to predict the cycle endurance. The predicted cycle endurance under these conditions can be seen in Fig. 14.

As the cycle predictions made here are based on data which was generated at peak temperatures of 240/250°C the life predictions which result should be considered as worst case endurance values. (As comparisons of the SN curves at different temperatures, show that cycle endurance is reduced when temperature increases).

This technique also allows the relative destructiveness of different cycling profiles to be compared. By calculating the equivalent cycling stress for each test scenario it is possible to reduce a two variable problem (peak temperature and temperature swing) into a single variable problem, facilitating the comparison of cases in which both the peak, and swing temperatures are varied.

#### VI. CONCLUSIONS

This paper presents a method which can be used to generate SN-curves based on experimental thermal cycling data obtained from test machines. This data allows the impact of thermal cycling on electric machines of a given construction to be considered. Furthermore, the use of Mean Stress Corrected values allows the two aspects of thermal cycling (peak temperature and temperature swing) to be combined into a single metric, allowing a range of different cycling profiles to be directly compared.

The combination of these two aspects makes this technique useful for gaining an insight into the effects of thermal cycling on an electric machine.

#### VII. ACKNOWLEDGMENT

The authors acknowledge the financial support from EPSRC for funding the research described in the paper under the Future Electrical Machines Manufacturing Hub (EPSRC EP/S018034/1).

#### VIII. REFERENCES

- [1] Z. Huang, A. Reinap and M. Alakula, "Degradation and fatigue of epoxy impregnated traction motors due to thermal and thermal induced mechanical stress - part I: Thermal mechanical simulation of single wire due to evenly distributed temperature," in *PEMD 2016*, Glasgow, UK, 2016.
- [2] Z. Huang, A. Reinap and M. Alakula, "Degradation and fatigue of epoxy impregnated traction motors due to thermal and thermal induced mechanical stress - part II: Thermal mechanical simulation of multiple wires due to evenly and unevenly distributed temperature," in *PEMD 2016*, Glasgow, UK, 2016.
- [3] P. Reis, J. Ferreira, J. Costa and M. Richardson, "Fatigue life evaluation for carbon/epoxy laminate composites under constant and variable block loading," *Composites Science and Technology*, vol. 69, no. 2, pp. 154-160, 2009.
- [4] Z. Lu, B. Feng and C. Loh, "Fatigue Behaviour and Mean Stress Effect of Thermoplastic Polymers and Composites," *Frattura ed Integrità Strutturale*, vol. 12, no. 46, pp. 150-157, 2018.
- [5] A. Griffio, I. Tsyokhla and J. Wang, "Lifetime of Machines Undergoing Thermal Cycling Stress," in *ECCE 2019*, Baltimore, MD, USA, 2019.
- [6] Z. Huang, Modeling and Testing of Insulation Degradation due to Dynamic Thermal Loading of Electrical Machines (PhD Thesis), Lund University, Sweden: Faculty of Engineering, Lund University, Sweden, 2017.
- [7] Solvay, Torlon PAI Design Guide V5.1, Solvay, 2020.